# Iterative Decomposition Algorithm for Electrical Impedance Tomography to Image Large Resistivity Changes

Haoting Li, Lei Li, Zhanqi Zhao, Meng Dai, Xiuzhen Dong, *Member, IEEE*, Bin Yang, and Feng Fu

***Abstract*—In electrical impedance tomography (EIT), the commonly used linear reconstruction algorithms are typically suitable for imaging small resistivity changes. However, in many applications of EIT, such as in imaging maximum ventilation of the lung with EIT, the resistivity changes can be very large. In such cases, the linear algorithms have reduced accuracy and may affect the image interpretation. To address this issue, a novel iterative decomposition algorithm (IDA) is developed. In IDA, the large resistivity change target is decomposed into small changes so that the final solution can be obtained through multiple linear reconstructions, and the sensitivity matrix is iteratively updated based on the result of each linear reconstruction. To test the performances of IDA, both simulation and in vivo experiments were conducted. The experimental results demonstrate that, in imaging large resistivity changes in lung ventilation, the traditional linear EIT algorithm caused nonnegligible linear approximation errors (LAEs) and location errors (LEs). For IDA, it could reduce LAEs and LEs by 13.4% and 11.6% respectively. The resistivity changes reconstructed by IDA had a better correlation with the lung volume changes. Therefore, IDA was verified as an efficient method for imaging large resistivity changes.**

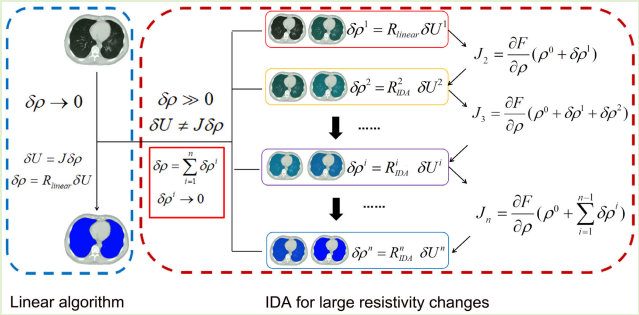


***Index Terms*— Electrical impedance tomography (EIT), image reconstruction algorithm, large resistivity changes, lung ventilation.**

## I. Introduction

ELECTRICAL impedance tomography (EIT) is a non-invasive, radiation-free, and low-cost method that can image the electrical property (resistivity or conductivity) distribution inside the human body using the sensor data obtained from surface electrodes [1], [2], [3]. It has been widely studied in lung, brain, and abdominal monitoring and was verified to have attractive clinical application prospects, such as monitoring regional lung ventilation at the bedside [4], [5], [6].

For EIT, high-quality imaging results are crucial for medical diagnosis; therefore, the performances of reconstruction algorithms in this field are of great importance. Researchers have proposed numerous EIT reconstruction algorithms, of which the linear EIT algorithms are the most popular [7]. The linear EIT algorithms typically assume the resistivity change of the target is very small; thus, the solution can be calculated by a global linearization of the observation model with a constant sensitivity matrix [8]. Because iterations are not required, linear EIT algorithms have the advantages of easy implementation and fast imaging.

However, in many applications of EIT, the resistivity changes can be very large. In maximum lung ventilation, a large volume of insulated air content is enclosed in the alveoli, enlarging its walls and significantly increasing the resistivity of the lung. According to previous studies, the change in lung resistivity at maximum ventilation is approximately 250% [9]. It was estimated that when the

Manuscript received 17 February 2024; revised 16 April 2024; accepted 18 April 2024. Date of publication 1 May 2024; date of current version 1 July 2024. This work was supported in part by the National Natural Science Foundation of China under Grant NSFC 52377230, in part by the Key Research and Development Plan of China under Grant 2022YFC2404800, and in part by the Key Research and Development Plan of Shaanxi Province under Grant 2022ZDLSF04-07. The associate editor coordinating the review of this article and approving it for publication was Dr. Marko Vauhkonen. *(Haoting Li and Lei Li contributed equally to this work.) (Corresponding authors: Feng Fu; Bin Yang.)*

This work involved human subjects or animals in its research. Approval of all ethical and experimental procedures and protocols was granted by the Ethics Committee of the Fourth Military Medical University under Application No. KY20234149-1, 2023-03-04.

Haoting Li, Lei Li, Meng Dai, Xiuzhen Dong, Bin Yang, and Feng Fu are with the Department of Biomedical Engineering, Fourth Military Medical University, Xi'an 710032, China (e-mail: binyang@fmmu.edu.cn; fengfu@fmmu.edu.cn).

Zhanqi Zhao is with the School of Biomedical Engineering, Guangzhou Medical University, Guangzhou 510180, China.

Digital Object Identifier 10.1109/JSEN.2024.3393938

filling factor (FF) of air content in lung tissue became 8, the resistivity change could reach about 12 Ω·m [10]. Furthermore, the shift of conductive fluids in the thorax and brain can also cause large resistivity changes [11].

For large resistivity changes, the linear EIT algorithms have reduced accuracy and may even become an obstacle for image interpretation. It was reported that the reconstructed large resistivity values tended to be underestimated with linear EIT algorithms [12]. Ngo et al. [13] utilized the linear EIT algorithm to map air volume changes during ventilation. They found that the reconstructed lung resistivity had a strictly linear relationship with air volume during normal ventilation, but inaccuracy appeared at the peak flow of maximum effort breathing [13]. Furthermore, because the sensitivity matrix in the EIT algorithm is determined by electromagnetic distribution and large resistivity changes can make electromagnetic distribution have evident changes, the use of a constant sensitivity matrix in linear EIT algorithms would also bring reconstruction errors [14], [15].

To improve the quality of imaging large resistivity changes, a novel EIT algorithm is proposed called the "iterative decomposition algorithm" (IDA). In IDA, the large resistivity changes of a target are decomposed into small changes so that the final solution can be calculated through multiple linear reconstructions, in which the sensitivity matrix is iteratively updated based on the results obtained in each linear reconstruction. To select the optimal iteration step, a method based on human electrical properties is proposed. Finally, simulation and in vivo experiments were conducted to compare the performances of IDA and traditional linear EIT algorithms in imaging large resistivity changes.

The remainder of this article is organized as follows: Sections II and III introduce the linear EIT algorithm and IDA. Section IV presents the experimental procedures for algorithm comparison. Section V gives the results of simulation and in vivo experiments. Section VI offers an analysis of the experimental results and discusses the performances of IDA. Section VII provides a brief conclusion.

## II. Linear EIT Algorithm

### A. Theory of Linear EIT Algorithm

EIT can reconstruct the resistivity changes $\delta\rho$ inside the human body. The mathematic model of EIT can be written as

$$\begin{cases} \delta\rho = \rho_{t2} - \rho_{t1} \\ U_{t1} = F(\rho_{t1}) + e_1 \\ U_{t2} = F(\rho_{t2}) + e_2 \end{cases} \tag{1}$$

where $\rho_{t1}$ and $\rho_{t2}$ are the resistivity distributions at two time instants. $U_{t1}$ and $U_{t2}$ are the measured boundary voltages. $F(\cdot)$ represents the forward operator which generates boundary voltages using the finite element method (FEM) [16]. $e_1$ and $e_2$ represent the Gaussian distributed measurement noise. With the Taylor series expansion method, (1) can be formulated as

$$\begin{aligned} U_{t1} &= F(\rho_0) + J(\rho_{t1} - \rho_0) + n(\rho_{t1} - \rho_0) + e_1 \\ U_{t2} &= F(\rho_0) + J(\rho_{t2} - \rho_0) + n(\rho_{t2} - \rho_0) + e_2 \end{aligned} \tag{2}$$

where $J = (\partial F/\partial\rho)(\rho_0)$ is the sensitivity matrix calculated at the initial resistivity estimate $\rho_0$ and $n(\cdot)$ represents the high-order derivative of the Taylor series.

By differencing $U_{t1}$ and $U_{t2}$, (2) can be written as

$$\delta U = J\delta\rho + n(\rho_{t1} - \rho_0) - n(\rho_{t2} - \rho_0) + e \tag{3}$$

where $\delta U = U_{t2} - U_{t1}$ is the boundary voltage changes, $e$ is the Gaussian distributed measurement noise. When $\rho_{t2} \approx \rho_0$ and $\rho_{t2} \approx \rho_0$, namely $\delta\rho$ is very small, (3) can be approximated as the linear equation

$$\delta U \approx J\delta\rho + e. \tag{4}$$

To solve $\delta\rho$, (4) is converted to the minimization problem

$$\delta\sigma = \arg\min\left(||\delta U - J\delta\sigma||^2 + \lambda P(\delta\sigma)\right) \tag{5}$$

where $\lambda$ is the regularization parameter and $P(\delta\sigma)$ is the regularization item. A popular regularization method is the L2 norm regularization method [17], which sets $P(\delta\rho)$ as $||\delta\rho||^2$. Therefore, $\delta\rho$ can be solved by

$$\delta\rho = (J^T J + \lambda I)^{-1} J^T \delta U = R_{\text{linear}}\delta U \tag{6}$$

where $\mathrm{R}_{\text{linear}}$ represents the linear reconstruction matrix.

### B. Linear Reconstruction Errors

As displayed in (4), in linear EIT algorithm, $\delta\rho$ is assumed to be very small, but when imaging large resistivity changes, the omission of high-order derivations of the Taylor series will cause reconstruction errors. In this study, we name it linear approximation errors (LAEs) and LAEs will become large with the increase in $\delta\rho$.

Further, the sensitivity matrix $J$ in the linear EIT algorithm is calculated at $\rho_0$ and kept constant in the reconstruction. But when $\delta\rho$ becomes very large, the electromagnetic field inside the human body will change significantly. In such case, the real sensitivity distribution will have a large difference from $J$. So, using the constant sensitivity matrix in a linear EIT algorithm will also cause reconstruction errors in imaging large resistivity changes.

## III. Iterative Decomposition Algorithm

To reduce the linear reconstruction errors, a novel IDA was developed.

### A. Theory of IDA

As shown in Fig. 1(a), IDA decomposes large resistivity changes into $n$ small ones, and the voltage change for the $i$th small resistivity changes $\delta\rho_i$ is

$$\delta U_i = \delta U/n, \quad i = 1, 2, 3, \ldots, n. \tag{7}$$

Because $\delta\rho_i$ is small, it satisfies the linear reconstruction

$$\delta\rho_i = R_{\text{linear}}\delta U_i. \tag{8}$$

As mentioned before, $R_{\text{linear}}$ that calculated with the constant sensitivity matrix $J$ will bring reconstruction errors. Thus, IDA iteratively updates the sensitivity matrix and calculates

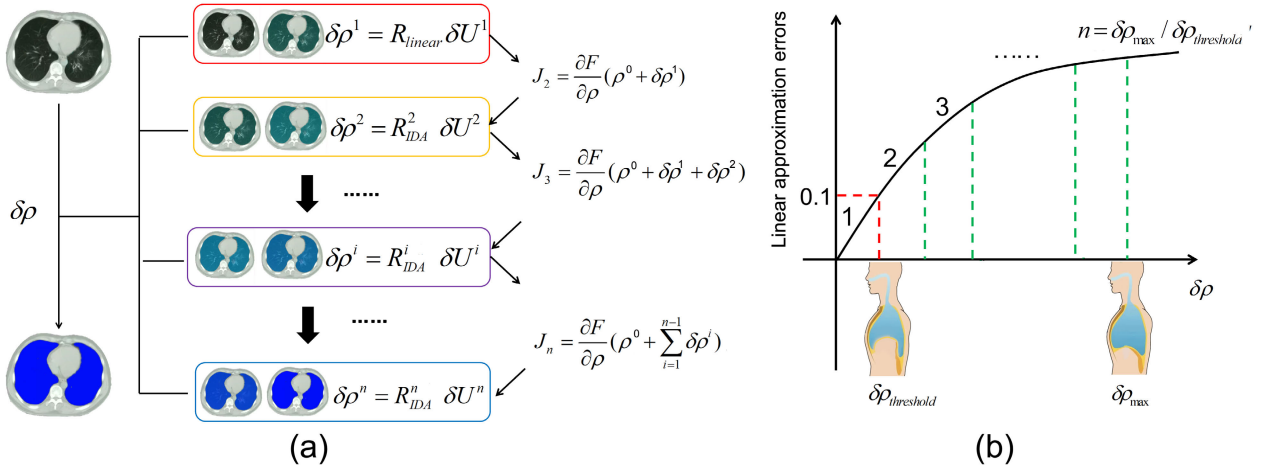


Fig. 1. Illustration of IDA. (a) Decomposing large resistivity changes into small changes for linear reconstructions. (b) Selecting the optimal iteration step based on electrical properties of lung.

the resistivity changes by

$$\begin{aligned} \rho_i &= \rho_{i-1} + \delta\rho_{i-1} \\ J_i &= \frac{\partial F}{\partial \rho}(\rho_i), \quad i = 2, 3, \ldots, n \\ \delta\rho_i &= \left(J_i^T J_i + \lambda J_i\right) J_i^T \delta U_i = R^i_{\mathrm{IDA}} \delta U_i \end{aligned} \tag{9}$$

where $R^i_{\mathrm{IDA}}$ $i = 2, 3, \ldots, n$ represents the reconstruction matrix of IDA and $R^1_{\mathrm{IDA}} = R_{\mathrm{linear}}$. Based on (9), the final solution can be obtained by

$$\delta\rho = \sum_{i=1}^{n} R^i_{\mathrm{IDA}} \delta U_i. \tag{10}$$

### B. Method for Selecting Optimal Iteration Step

In IDA, the iteration step $n$ is crucial because it determines the reconstruction accuracy and speed. As shown in Fig. 1(b), a human electrical property prior information-based method was proposed for selecting the optimal $n$.

*1) Estimating the Maximum Lung Resistivity Changes:* According to previous studies, the resistivity of lung tissue at different ventilation states can be estimated as

$$\rho = \frac{\bar{\tau}}{\sigma_{\mathrm{Alv}}}(\mathrm{FF} + 1) \tag{11}$$

where $\bar{\tau} = 1.71, \bar{\tau} = 1.71\sigma_{\mathrm{Alv}} = 0.7284\ \Omega^{-1}\mathrm{m}^{-1}$ and the physiological FF is usually in the range of 2.0–6.0 [10]. So, the maximum resistivity change $\delta\rho_{\max}$ in lung ventilation is approximately 9.4 Ω·m.

*2) Defining the Threshold for Linear Reconstructions:* The threshold for linear reconstructions is empirically defined as the resistivity changes that make LAEs increase to 10%. Based on the results of the following simulation experiments, $\delta\rho_{\mathrm{threshold}}$ is approximately 3 Ω·m.

*3) Determining the Optimal Iteration Step for IDA:* To satisfy the linear reconstruction, the resistivity changes in each iteration step should be no more than $\delta\rho_{\mathrm{threshold}}$. So, the optimal iteration step for IDA can be determined as

$$n_{\mathrm{optimal}} = \delta\rho_{\max}/\delta\rho_{\mathrm{threshold}} \tag{12}$$

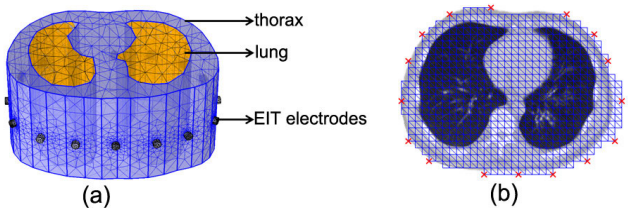


Fig. 2. Simulation models. (a) Three-dimensional lung simulation model with EIT electrodes. (b) Two-dimensional lung simulation model for EIT image reconstruction.

where $n_{\mathrm{optimal}}$ represents the optimal iteration step and $n_{\mathrm{optimal}} = 9.4/3 \approx 3$.

## IV. Experimental Procedures

To validate the performance of IDA in reconstructing large resistivity changes, both simulation and in vivo experiments are conducted and the experimental procedures are introduced in this section.

### A. Simulation Experiments

*1) Generation of Simulation EIT Data:* As displayed in Fig. 2(a), a 3-D lung model is used to simulate large resistivity changes and generate EIT data in this study. It consists of 44 064 elements and has real anatomical geometric boundaries. The resistivity values of different lung structures are set according to the dielectric properties of lung tissues reported in previous studies [18]. Sixteen Ag/AgCl EIT electrodes are uniformly placed on the boundary of the model. Adjacent patterns are used for excitation and measurement [19]. With the 3-D model, one can alter the lung resistivity to simulate large resistivity changes during ventilation. Fig. 2(b) shows the matched 2-D lung model for EIT image reconstruction.

*2) Algorithm Evaluation Metrics:* LAEs, location errors (LEs), and mean reconstruction speed (MIS) are introduced to evaluate the performances of different EIT algorithms in imaging large resistivity changes.

Fig. 3. Measurement systems. (a) EIT hardware. (b) Lung function tester.

Referring to [12], without measurement noise, LAEs can be calculated as

$$\text{LAEs} = n(\delta\rho) = (\delta U - J\delta\rho)/\delta U \tag{13}$$

where $n(\delta\rho)$ represents the high-order derivations in the Taylor series.

LEs can be calculated as

$$\text{LEs} = \frac{d}{l} \tag{14}$$

where $d$ represents the distance between the reconstructed and predefined resistivity changes. $l$ represents the length of the long axis of the reconstruction model.

MIS is defined as the mean time required for per image reconstruction and can be calculated as

$$\text{MIS} = \left(\sum_{i=1}^{m} t_i\right) \Big/ m \tag{15}$$

where $m$ is the total number of reconstructions and $t_i$ represents the time for the $i$th reconstruction.

### B. In Vivo Experiments

*1) Measurement Systems:* In in vivo experiments, EIT measurements are obtained by PulmoVista 500 (Drager Medical) EIT device [20] shown in Fig. 3(a). Lung volume changes are recorded by Ruichao-ST (Keluode Health) cardiopulmonary function tester shown in Fig. 3(b).

*2) In Vivo Experimental Protocols:* Three healthy volunteers (three males, aged 26–38) were recruited for the in vivo experiments. Participants were asked to inhale deeply at a constant speed. Lung resistivity changes were obtained by EIT and the lung volume changes were recorded by the cardiopulmonary function tester. Each measurement was performed three times. Then the correlations between ARV obtained by different algorithms and lung volume changes were compared. The experiment was conducted in accordance with the Declaration of Helsinki, and approved by the ethics committee of the Fourth Military Medical University (KY20234149-1, 2023-03-04).

## V. Results

### A. Results of Simulation Experiments

*1) Comparison of LAEs:* Fig. 4 shows the results of experiment one, in which the LAEs of different algorithms in imaging large resistivity changes were compared. In Fig. 4(a), based on the 3-D lung model, lung shape targets were simulated with resistivity changes ranging from 1 to 10 Ω·m. Fig. 4(b) and (c) are the reconstructed images of different algorithms and their corresponding LAEs. For EIT images reconstructed by linear algorithm, the color of lung area changed gradually with the increase of resistivity. However, as shown in the red dotted box, when $\delta\rho$ went from 8 to 10 Ω·m, the images reconstructed by linear algorithm had little difference, possibly causing an inaccurate estimation that that there were no changes in the lung. Compared with the linear algorithm, IDA could reflect the large resistivity changes better and reduce LAEs by approximately 13.4%. Fig. 4(d) shows the normalized average reconstructed value (ARV) of the above imaging results and their correlation indexes. ARV is calculated by averaging the reconstructed values of all mesh elements. The greed line represents the ideal ARV that changes linearly with the true values. The blue line is the ARV obtained by linear EIT algorithm, and its linearity was reduced when $\delta\rho$ became very large. The red line is the ARV obtained by IDA. It had better linearity in mapping large resistivity and better correlation with the ideal ARV.

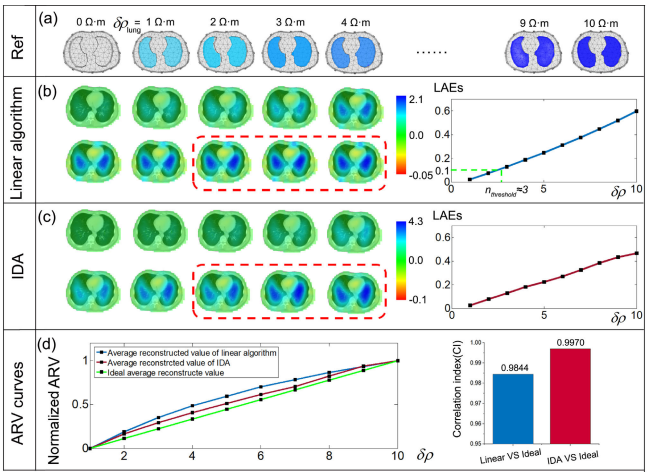


Fig. 4. Results of experiment 1. (a) Reference images with lung resistivity changes from 1 to 10 Ω·m. (b) and (c) EIT images and LAEs obtained by linear EIT algorithm and IDA. The red boxes show the imaging results with large resistivity changes. (d) Normalized ARV of the above imaging results and their correlation indexes with the ideal ARV.

*2) Comparison of Les:* Fig. 5 shows the results of experiment two, in which the LEs of different algorithms in imaging large resistivity changes were compared. In Fig. 5(a), the resistivity change of the spherical target was set as −1 Ω·m, while the resistivity change of the lung shaped target could be tuned from 1 to 10 Ω · m. Fig. 5(b) and (c) are the imaging results obtained by linear EIT algorithm and IDA. Because the resistivity change and size of the spherical target were much smaller than those of lung-shaped target, the reconstructed spherical target could not be observed based on the original imaging results. To solve this problem, a mask which set the resistivity values in lung area as 0 was used to highlight the location of the spherical target. From the results, we could see that when lung resistivity changes became very large,

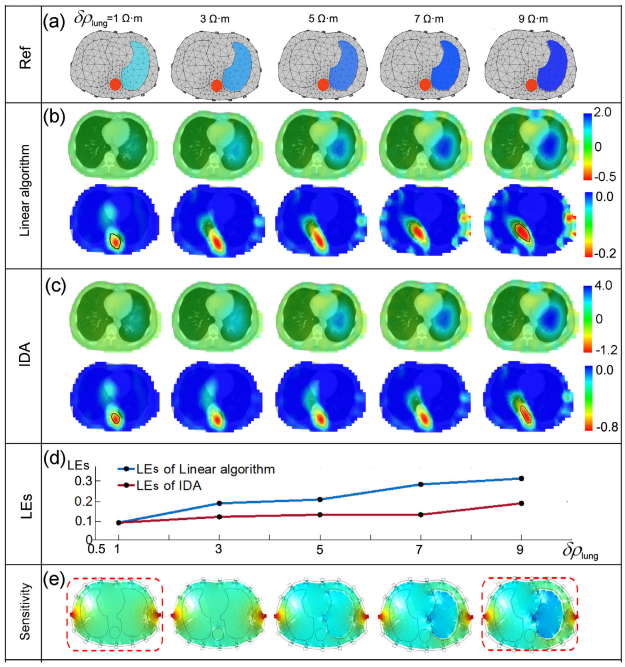


Fig. 5. Results of experiment 2. (a) Reference images with large resistivity changes. (b) and (c) EIT images obtained by linear algorithm and IDA. The reconstructed values in lung area were set as 0 to highlight the spherical targets. (d) LEs of images obtained by linear algorithm and IDA.

the reconstructed spherical target had increased LEs. Fig. 5(d) shows the LEs of reconstruction results obtained by different algorithms. Compared with the linear algorithm, IDA reduced LEs by approximately 11.6%. Fig. 5(e) shows the current distributions of the lung with different resistivity changes. As displayed in the red dotted boxes, the current distribution of the lung with large resistivity changes had evident difference from that at the initial state. For the linear EIT algorithm, it usually uses the constant sensitivity matrix calculated based on the initial current distribution, so its imaging results had increased LEs. While for IDA, it updates the sensitivity matrix based on the result in each iteration calculation. Therefore, IDA could improve the location accuracy of large resistivity changes. Our results are consistent with those reported by Liston [14].

*3) Comparison of MIS:* The mean imaging speed of the linear EIT algorithm and IDA were compared based on the desktop computer with a 4.2 GHz CPU and 16 G RAM. The MIS of the linear algorithm was approximately 0.005 s while that of IDA was approximately 324 s. The results indicate that IDA improved the image quality of large resistivity changes by sacrificing imaging speed.

### B. Results of In Vivo Experiments

Fig. 6 shows the representative results of in vivo experiments. As displayed in Fig. 6(a), volunteers were asked to try to inhale deeply at a constant speed. Then, EIT and the cardiopulmonary function tester were used to record resistivity changes and volume changes of the lung simultaneously. Fig. 6(b) shows the EIT images obtained by linear and IDA algorithm. Similar to the simulation results, the in vivo experiment results demonstrate that, compared with the traditional linear algorithm, IDA could reflect large resistivity changes of lung better. In Fig. 6(c), the lung volume changes and ARV curves obtained by different algorithms are plotted. Fig. 6(d) shows the results of correlation analysis between ARV curves and lung volume changes. The results demonstrate that ARV curves obtained by IDA had better correlation with the lung volume changes, especially near the peak of the inhalation. Therefore, compared with the linear EIT algorithm, IDA can reconstruct large resistivity changes in lung ventilation with better accuracy.

## VI. Discussion

In this study, the influences of the traditional linear EIT algorithm on the imaging accuracy of large resistivity changes were investigated, and a novel algorithm, IDA, was developed to improve the image quality.

### A. Influences of Linear EIT Algorithm in Imaging Large Resistivity Changes

First, as shown in experiment one, LAEs of the linear EIT algorithm become nonnegligible when imaging large resistivity changes. This error reduces the linearity between the reconstructed and true resistivity changes, and may even cause an inaccurate estimation of the ventilation state. Second, large resistivity changes cause evident changes in the electromagnetic field. Using the constant sensitivity matrix determined by the initial resistivity distribution in a linear EIT algorithm would result in increased LEs.

### B. Performances of IDA in Imaging Large Resistivity Changes

The proposed IDA, which decomposes the large resistivity changes into smaller ones and updates the sensitivity coefficient matrix based on the results of each linear reconstruction, reduced LAEs and LEs. The imaging results of the IDA demonstrated a better correlation with large resistivity changes in lung ventilation. However, its reconstruction speed was insufficient for real-time imaging. Therefore, using the IDA for offline image reconstruction and data analysis of large resistivity changes is recommended.

In addition to monitoring lung ventilation, many other EIT applications have large resistivity changes, such as monitoring the dehydration treatment of patients with brain edema and evaluating large volume changes of the bladder [11], [21]. In these applications, the IDA may also be used to improve image reconstruction quality.

### C. Performances of IDA in Imaging Small Resistivity Changes

In imaging small changes that satisfy the linear reconstruction conditions, the decomposition step of IDA will become unnecessary. It will only slow down the imaging speed without reducing the linear reconstruction errors. And because the small resistivity changes will not significantly change the electromagnetic distribution inside the lung, there is no need to update the sensitivity matrix. Therefore, in imaging small changes, IDA will get results similar to those obtained

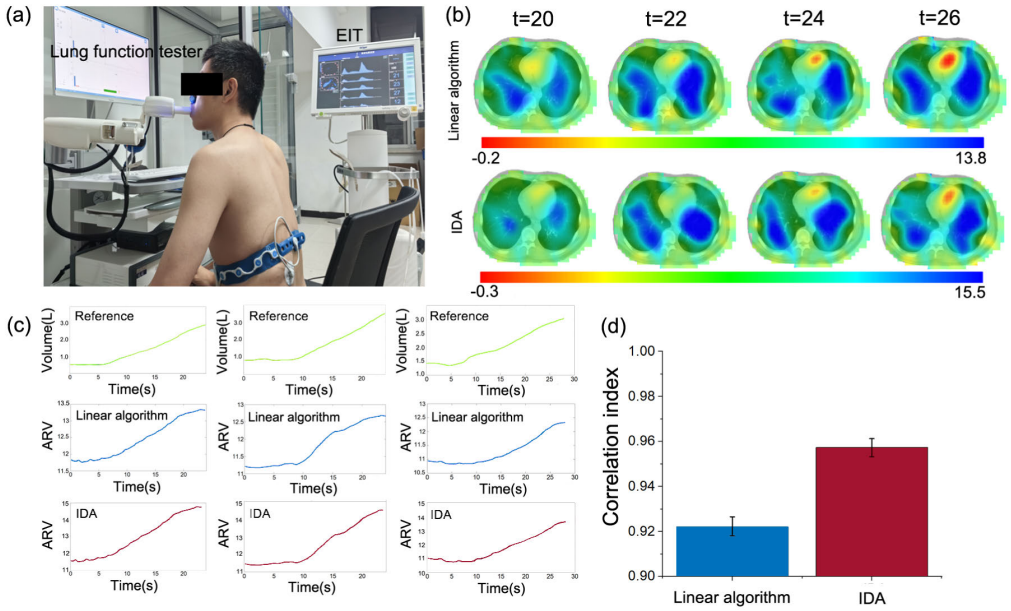


Fig. 6. Results of in vivo experiments. (a) Photograph of imaging maximum lung ventilation with EIT and cardiopulmonary function tester. (b) EIT images of maximum lung ventilation obtained by linear algorithm and IDA. (c) Lung volume changes and ARV curves obtained by different algorithms. (d) Correlation indexes between ARV curves and lung volume changes.

by linear algorithm, but its imaging speed is much lower. Therefore, IDA is not recommended for imaging small resistivity changes.

### D. Other Statements

Finally, several points should be noted. First, GREIT is a more popular linear EIT algorithm in imaging lung ventilation [7] but was not used for comparison in this study because GREIT has a similar mathematical model to the L2 norm regularization algorithm [22]; therefore, the capacity and errors of the two algorithms in reconstructing large resistivity changes would be similar. GREIT incorporates image-processing techniques, which may cause unfair algorithm comparisons. Second, the imaging linearity of the linear EIT algorithm was reduced when resistivity changes became very large. Besides the LAEs, this error may be related to the use of 2-D EIT images to reflect 3-D resistivity changes. And this problem may be investigated and solved by training a better reconstruction algorithm based on machine learning [23] in the future.

## VII. Conclusion

In reconstructing large resistivity changes in lung ventilation, the traditional linear EIT algorithm with the constant sensitivity matrix caused linear reconstruction errors. The proposed IDA could reduce the above errors, and enable the reconstruction results to have a better correlation with large resistivity changes in lung ventilation. Therefore, IDA is an efficient method for imaging large resistivity changes.

## References

[1] R. Bayford and A. Tizzard, "Bioimpedance imaging: An overview of potential clinical applications," *Analyst*, vol. 137, no. 20, pp. 4635–4643, 2012, doi: 10.1039/c2an35874c.

[2] T. J. Noble, N. D. Harris, A. H. Morice, P. Milnes, and B. H. Brown, "Diuretic induced change in lung water assessed by electrical impedance tomography," *Physiological Meas.*, vol. 21, no. 1, pp. 155–163, Feb. 2000, doi: 10.1088/0967-3334/21/1/319.

[3] X.-Y. Ke et al., "Advances in electrical impedance tomography-based brain imaging," *Mil. Med. Res.*, vol. 9, no. 1, p. 10, Dec. 2022, doi: 10.1186/s40779-022-00370-7.

[4] R. H. Bayford, "Bioimpedance tomography (electrical impedance tomography)," *Annu. Rev. Biomed. Eng.*, vol. 8, no. 1, pp. 63–91, Aug. 2006, doi: 10.1146/annurev.bioeng.8.061505.095716.

[5] I. Frerichs et al., "Chest electrical impedance tomography examination, data analysis, terminology, clinical use and recommendations: Consensus statement of the translational EIT developmeNt stuDy group," *Thorax*, vol. 72, no. 1, pp. 83–93, Jan. 2017, doi: 10.1136/thoraxjnl-2016-208357.

[6] A. Adler and A. Boyle, "Electrical impedance tomography: Tissue properties to image measures," *IEEE Trans. Biomed. Eng.*, vol. 64, no. 11, pp. 2494–2504, Nov. 2017, doi: 10.1109/TBME.2017.2728323.

[7] A. Adler et al., "GREIT: A unified approach to 2D linear EIT reconstruction of lung images," *Physiological Meas.*, vol. 30, no. 6, pp. 35–55, Jun. 2009, doi: 10.1088/0967-3334/30/6/s03.

[8] D. Liu, V. Kolehmainen, S. Siltanen, and A. Seppänen, "A nonlinear approach to difference imaging in EIT; Assessment of the robustness in the presence of modelling errors," *Inverse Problems*, vol. 31, no. 3, Mar. 2015, Art. no. 035012, doi: 10.1088/0266-5611/31/3/035012.

[9] C. J. Roth et al., "Correlation between alveolar ventilation and electrical properties of lung parenchyma," *Physiological Meas.*, vol. 36, no. 6, pp. 1211–1226, Jun. 2015, doi: 10.1088/0967-3334/36/6/1211.

[10] P. Nopp, E. Rapp, H. Pfutzner, H. Nakesch, and C. Rusham, "Dielectric properties of lung tissue as a function of air content," *Phys. Med. Biol.*, vol. 38, no. 6, pp. 699–716, Jun. 1993, doi: 10.1088/0031-9155/38/6/005.

[11] B. Yang et al., "Comparison of electrical impedance tomography and intracranial pressure during dehydration treatment of cerebral edema," *NeuroImage, Clin.*, vol. 23, Jan. 2019, Art. no. 101909.

[12] N. Polydorides, "Linearization error in electrical impedance tomography," *Prog. Electromagn. Res.*, vol. 93, pp. 323–337, 2009, doi: 10.2528/pier09052503.

[13] C. Ngo et al., "Linearity of electrical impedance tomography during maximum effort breathing and forced expiration maneuvers," *Physiological Meas.*, vol. 38, no. 1, pp. 77–86, Jan. 2017, doi: 10.1088/1361-6579/38/1/77.

[14] A. D. Liston, R. H. Bayford, and D. S. Holder, "The effect of layers in imaging brain function using electrical impedance tomograghy," *Physiological Meas.*, vol. 25, no. 1, pp. 143–158, Feb. 2004, doi: 10.1088/0967-3334/25/1/022.
[15] H. Li et al., "Unveiling the development of intracranial injury using dynamic brain EIT: An evaluation of current reconstruction algorithms," *Physiological Meas.*, vol. 38, no. 9, pp. 1776–1790, Aug. 2017, doi: 10.1088/1361-6579/aa8016.
[16] M. Jehl, A. Dedner, T. Betcke, K. Aristovich, R. Klöfkorn, and D. Holder, "A fast parallel solver for the forward problem in electrical impedance tomography," *IEEE Trans. Biomed. Eng.*, vol. 62, no. 1, pp. 126–137, Jan. 2015, doi: 10.1109/TBME.2014.2342280.
[17] C. Xu et al., "An optimized strategy for real-time hemorrhage monitoring with electrical impedance tomography," *Physiological Meas.*, vol. 32, no. 5, pp. 585–598, May 2011.
[18] W. R. Fan and H. X. Wang, "3D modelling of the human thorax for ventilation distribution measured through electrical impedance tomography," *Meas. Sci. Technol.*, vol. 21, no. 11, Nov. 2010, Art. no. 115801, doi: 10.1088/0957-0233/21/11/115801.
[19] A. Adler, P. O. Gaggero, and Y. Maimaitijiang, "Adjacent stimulation and measurement patterns considered harmful," *Physiological Meas.*, vol. 32, no. 7, pp. 731–744, Jul. 2011, doi: 10.1088/0967-3334/32/7/s01.
[20] R. L. Parke, A. Bloch, and S. P. McGuinness, "Effect of very-high-flow nasal therapy on airway pressure and end-expiratory lung impedance in healthy volunteers," *Respiratory Care*, vol. 60, no. 10, pp. 1397–1403, Oct. 2015, doi: 10.4187/respcare.04028.
[21] B. M. G. Rosa and G. Z. Yang, "Bladder volume monitoring using electrical impedance tomography with simultaneous multi-tone tissue stimulation and DFT-based impedance calculation inside an FPGA," *IEEE Trans. Biomed. Circuits Syst.*, vol. 14, no. 4, pp. 775–786, Aug. 2020, doi: 10.1109/TBCAS.2020.3008831.
[22] B. Grychtol, B. Müller, and A. Adler, "3D EIT image reconstruction with GREIT," *Physiological Meas.*, vol. 37, no. 6, pp. 785–800, Jun. 2016, doi: 10.1088/0967-3334/37/6/785.
[23] L. Zhu, W. Lu, M. Soleimani, Z. Li, and M. Zhang, "Electrical impedance tomography guided by digital twins and deep learning for lung monitoring," *IEEE Trans. Instrum. Meas.*, vol. 72, pp. 1–9, 2023, doi: 10.1109/TIM.2023.3298389.

**Haoting Li** received the B.S., M.S., and Ph.D. degrees in biomedical engineering from the Fourth Military Medical University, Xi'an, China, in 2014, 2017, and 2020, respectively. He is currently pursuing the Postdoctoral degree with Fourth Military Medical University, under the supervision of Prof. F. Fu.

His research interests include biomedical electrical impedance tomography, biomedical signal processing, and inverse problems.

**Lei Li**, photograph and biography not available at the time of publication.

**Zhanqi Zhao**, photograph and biography not available at the time of publication.

**Meng Dai**, photograph and biography not available at the time of publication.

**Xiuzhen Dong** (Member, IEEE) was born in Beijing, China, in 1945. She received the B.S. degree in automatic control from Harbin Military Engineering University, Harbin, China, in 1968.

Since 1994, she has been a Professor with Fourth Military Medical University, Xi'an, China, where she has also been a Doctoral Advisor, since 1998. She has authored or coauthored more than 200 papers published in international journals and conferences. Her current research interests include electrical impedance tomography and biomedical signal detection and processing.

**Bin Yang**, photograph and biography not available at the time of publication.

**Feng Fu** received the B.S., M.S., and M.D. degrees in biomedical engineering from Fourth Military Medical University, Xi'an, China, in 1993, 1996, and 1999, respectively.

He is currently a Professor at the Department of Biomedical Engineering, Fourth Military Medical University. His current research interests include electrical impedance measurement and imaging.